Supporting Information for

Polyglutamine amyloid core boundaries and flanking domain dynamics in huntingtin fragment fibrils determined by solid-state NMR

Cody L. Hoop, Hsiang-Kai Lin, Karunakar Kar, Zhipeng Hou, Michelle A Poirier, Ronald Wetzel, and Patrick C.A. van der Wel

Department of Structural Biology, University of Pittsburgh School of Medicine, Biomedical Science Tower 3, 3501 Fifth Ave, Pittsburgh, Pennsylvania 15260, USA

Division of Neurobiology, Department of Psychiatry, Children's Medical Surgical Center, Johns Hopkins University School of Medicine, Baltimore, MD 21287, USA

Table S1- Detailed experimental conditions *of NMR experiments shown in the main text and SI. Abbreviations: NS, number of scans per t_1 point; Temp., temperature; MAS, magic angle spinning rate; RD, recycle delay; TPPM, ^1H decoupling power during evolution and acquisition (using two-pulse phase modulation scheme).*

1D Spectra									
Fig.	**Sample (refer to Table 1 in main text)**	**Experiment**	**NS**	**Temp (K)**	**MAS (kHz)**	**RD (s)**	**TPPM during acq. (kHz)**	**T_2 filter time (ms)**	**^1H-^1H Mixing (ms)**
2a, 3a,d, S1	LQP-labeled	^1H-^{13}C CP	1024	275	9.8	2.8	83	NA	NA
2b	$htt^{NT}Q_{30}P_{10}K_2$ *	^1H-^{13}C CP	2662	275	10	3	83	NA	NA
3b,c	LQP-labeled	^1H T_2 filter	3072	275	9.8	2.8	83	3.0	0
3c	LQP-labeled	^1H T_2 filter	3072	275	9.8	2.8	83	3.0	1
3c	LQP-labeled	^1H T_2 filter	3072	275	9.8	2.8	83	3.0	2
3c	LQP-labeled	^1H T_2 filter	3072	275	9.8	2.8	83	3.0	3
3c	LQP-labeled	^1H T_2 filter	3072	275	9.8	2.8	83	3.0	4
3b,c	LQP-labeled	^1H T_2 filter	3072	275	9.8	2.8	83	3.0	7
3d	LQP-labeled	^1H-^{13}C DP	1024	275	9.8	2.8	83	NA	NA
5a	MA-labeled	^{15}N T_1	1024	315	22	3	83	NA	NA
5a	MA-labeled	^{15}N T_1	1024	273	19	3	83	NA	NA
5b	[U-^{13}C,^{15}N-Q10]-$K_2Q_{11}PGQ_{11}D_2$	^{15}N T_1	790	275	22	6	83	NA	NA
5c,d	MA-labeled	N-H dipolar coupling	2048	287	10	3	83	NA	NA
5c,d	MA-labeled	N-H dipolar coupling	2048	250	10	3	83	NA	NA
5e	[U-^{13}C,^{15}N-Q10]-$K_2Q_{11}PGQ_{11}D_2$	N-H dipolar coupling	2048	275	10	3	83	NA	NA
6a	1:1 MF-labeled/LAQ-labeled	^1H-^{13}C CP	256	287	9.8	3	83	NA	NA
6a	1:1 MF-labeled/LAQ-labeled	^1H-^{13}C DP	256	287	9.8	3	83	NA	NA
6b	1:1 MF-labeled/LAQ-labeled	^1H-^{13}C CP	256	265	9.8	3	83	NA	NA
6b	1:1 MF-labeled/LAQ-labeled	^1H-^{13}C DP	256	265	9.8	3	83	NA	NA
6c	1:1 MA-labeled/LQP-labeled	^1H-^{13}C CP	256	287	9.8	3	83	NA	NA
6c	1:1 MA-labeled/LQP-labeled	^1H-^{13}C DP	256	287	9.8	3	83	NA	NA
6d	1:1 MA-labeled/LQP-labeled	^1H-^{13}C CP	256	270	9.8	3	83	NA	NA
6d	1:1 MA-labeled/LQP-labeled	^1H-^{13}C DP	256	270	9.8	3	83	NA	NA
S1b	LKSQ-labeled	^1H-^{13}C CP	4096	275	13	3.5	83	NA	NA
S1b	LKSQ-labeled	^1H-^{13}C DP	4096	275	13	3.5	83	NA	NA

* Natural abundance signals from $htt^{NT}Q_{30}P_{10}K_2$ aggregates that lacked isotopic labeling.

2D Spectra									
Fig.	**Sample (refer to Table 1 in main text)**	**Experiment**	**NS**	**Temp (K)**	**MAS (kHz)**	**RD (s)**	**TPPM during acq. (kHz)**	**t_1 evol. (μs)**	**Mixing (ms)**
1a	LQP-labeled	DARR 2D	64	275	9.8	2.8	83	422x33.11	8
1b	LQP-labeled	DARR 2D	72	275	9.8	2.8	83	370x36.78	15
1c	LAQ-labeled	DARR 2D	128	276	10	2.8	83	240x36.78	8
1d	LKSQ- labeled	DARR 2D	96	275	13	3	83	832x19.23	25
4a,b, S2	U-^{13}C,^{15}N-htt exon 1	DARR 2D	256	275	10	2.6	83	448x35.60	15
4b, S2	LQP-labeled	DARR 2D	72	275	9.8	2.8	83	370x36.78	15
4b, S2	LKSQ- labeled	DARR 2D	96	275	13	3	83	832x19.23	25
S3a	MA-labeled	DARR 2D	64	275	10	2.8	83	422x33.1	8

Table S2 - ^{13}C and ^{15}N chemical shift assignments of residues isotopically labeled in htt$^{NT}Q_{30}P_{10}K_2$ peptide fibrils, *from this study and from previously published work [1]. The uncertainty in the chemical shifts is ± 0.1-0.3 ppm unless otherwise stated. ^{13}C referencing is relative to aqueous DSS (see Experimental Procedures section). These data are also available online at the Biological Magnetic Resonance Data Bank (BMRB), via BMRB accession number 25146.*

Res.[a)]	C'	Cα	Cβ	Cγ	Cδ(1)	Cδ2	Cε	N	Nε2
A2	178.2	52.7	19.1						
L4	178.4	58.0	41.4	27.0	25.3	24.2			
K6	179.9	59.5	32.6	25.8	29.6		42.1		
L7	178.0	57.9	42.0	26.9	25.2	24.0		121.6	
M8	178.9	58.0	32.1	32.3			17.0	118.7	
A10	180.3	55.0	18.0					123.2	
F11	-	61.2	39.3	131.4					
L14	177.0 ± 0.4	55.7 ± 0.4	42.1	26.6	26.6	23.3			
S16a	173.0 ± 0.5	56.8	65.2						
S16b	173.0 ± 0.5	58.9	62.8						
F17a	175.8	57.1	-	131.7					
F17b	174.3	56.6	-	131.7					
Q18a	175.6	55.7	34.2	34.4	178.8				
Q18b	174.2	54.7	30.9	30.7	177.8				
Q19a	176.0	56 .0	34.2	34.2	178.6				
Q19b	174.2	53.9	31.1 ± 0.4	30.6	177.6				
Q46a	175.1	56.0	34.3	34.0	178.7				
Q46b	174.2	54.1	31.6	30.2	178.3				
Q46c	-	-	-	34.1	179.8				
Q47c1	172.5	53.7	29.1	33.4	180.4			123.1	111.4
Q47c2	173.0 ± 0.5	53.0	30.3	34.3	178.6			117.7	107.7
P48	174.2	61.3	30.5	27.3	50.5			136 ± 1	
Pro NA	-	61.2	30.6	26.8	50.3				

a) For residues with multiple detected conformers, lower-case letters indicate the conformers.

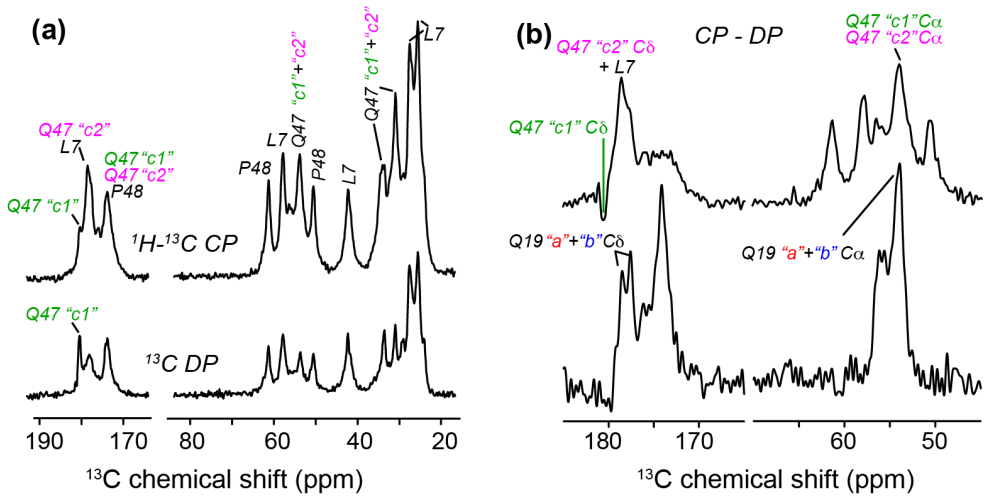

Figure S1. *Mobility at the Q/P junction. (a) Comparison of ^{1}H-^{13}C CP (top) and ^{13}C DP (bottom) 1D MAS ssNMR spectra on the LQP-labeled fibrils at 9.8 kHz MAS. Q47 peaks are indicated and color-coded by conformer "c1" (green) and "c2" (magenta). (b) CP-DP difference spectra for fibrils from LQP- (top) and LKSQ-labeled (13 kHz MAS) (bottom) fibrils. High intensity peaks in these difference spectra indicate increased rigidity. Q47 is less rigid than Q19 in the polyQ core, with especially pronounced mobility for the side chain carbonyl group (Cδ) of conformer "c1". Several Q47 side chain peaks, e.g. the c1 Cδ (far left in (a)) or the Cβ/Cγ signals in Fig. 3d, are also significantly narrower, indicative of fast side-chain motion.*

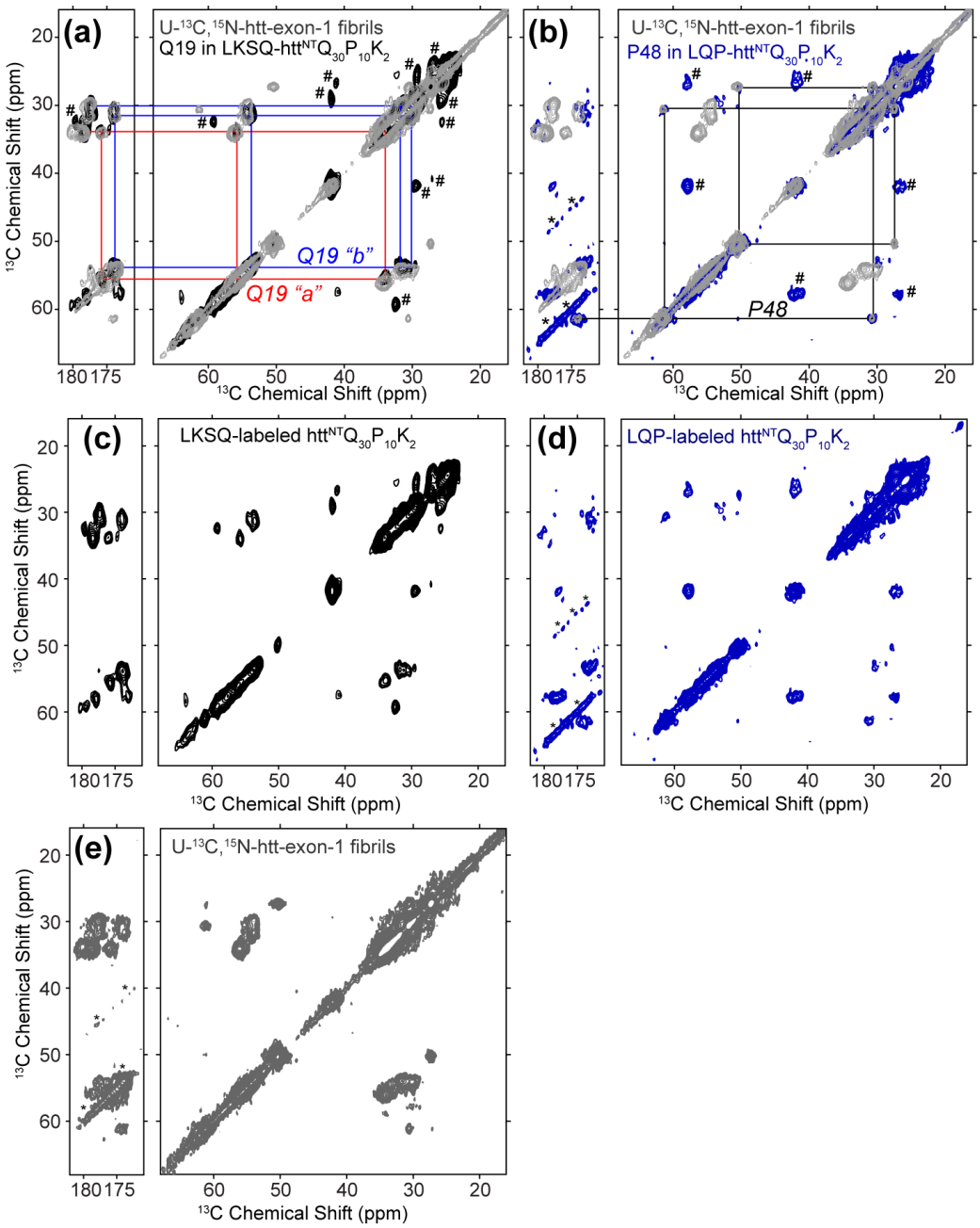

Figure S2. *Comparison of the signals from polyQ and PRD in U-^{13}C,^{15}N htt exon 1 fibrils and residue-specific labels in htt$^{NT}Q_{30}P_{10}K_2$ fibrils. (a) Overlay of htt exon-1 (grey) and LKSQ-labeled htt$^{NT}Q_{30}P_{10}K_2$ fibrils; Q19 conformers "a" and "b" are marked. (b) Overlay of htt exon-1 (grey) and LQP-labeled htt$^{NT}Q_{30}P_{10}K_2$ fibrils; P48 signals are marked. (c-d) Individual spectra for the htt$^{NT}Q_{30}P_{10}K_2$ fibrils used in the overlays in Fig. 4 and this figure. (e) The ^{13}C-^{13}C 2D spectrum of U-^{13}C,^{15}N-labeled fibrils by itself; shown with lower contour levels close to the noise level. Experimental details are in Table S1 and the main text.*

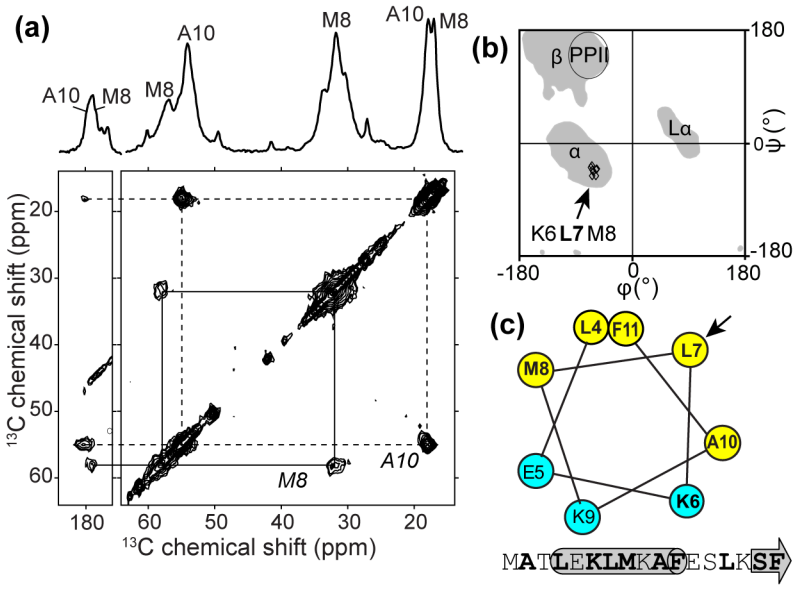

Figure S3. *(a) 1D and 2D MAS ssNMR spectra obtained on MA-labeled htt^{NT}Q$_{30}$P$_{10}$K$_2$ fibrils. Bottom: aliphatic/carbonyl (vertical section on left) and intra-aliphatic (right) regions of a 2D ^{13}C-^{13}C spectrum obtained with 8ms DARR mixing. Both spectra were acquired at 600MHz (^{1}H freq.) and 10 kHz MAS. (b) Ramachandran plot of the backbone torsion angles for L7 (black diamonds) based on the TALOS+ analysis of the chemical shifts of K6, L7, and M8. (c) Helical wheel plot of the α-helix within htt^{NT} with ssNMR-probed residues in bold, hydrophilic residues shown in cyan and hydrophobic residues in yellow. Residue L7 (arrow) (labeled here and in ref. [1]) forms the middle of the hydrophobic face, and is thus expected to form part of a hydrophobic "core" upon clustering of the amphipathic α-helices.*

References Cited in the Supporting Information

1. Sivanandam, V. N.; Jayaraman, M.; Hoop, C. L.; Kodali, R.; Wetzel, R.; van der Wel, P. C. A., The aggregation-enhancing huntingtin N-terminus is helical in amyloid fibrils. *J Am Chem Soc* **2011,** *133* (12), 4558-4566.